Geophysical Research Letters

RESEARCH LETTER
10.1029/2018GL080045

**Key Points:**
- Model and field results show that shutter ridges are essential for sustaining fault-parallel stream channel offsets along strike-slip faults
- Channel offset length is primarily controlled by the length scale of shutter ridges, regardless of total lateral fault offset
- Frequency of strike-slip-induced stream capture is affected by shutter ridge dimensions, as well as by the fault slip rate

**Supporting Information:**
- Supporting Information S1
- Data Set S1
- Movie S1
- Movie S2
- Movie S3
- Movie S4
- Movie S5

**Correspondence to:**
S. A. Harbert,
harbert1@uw.edu

**Citation:**
Harbert, S. A., Duvall, A. R., & Tucker, G. E. (2018). The role of near-fault relief elements in creating and maintaining a strike-slip landscape. *Geophysical Research Letters*, *45*, 11,683–11,692. https://doi.org/10.1029/2018GL080045

Received 13 AUG 2018
Accepted 16 OCT 2018
Accepted article online 19 OCT 2018
Published online 7 NOV 2018



# The Role of Near-Fault Relief Elements in Creating and Maintaining a Strike-Slip Landscape

**S. A. Harbert**[1], **A. R. Duvall**[1], **and G. E. Tucker**[2,3]

[1]Department of Earth and Space Sciences, University of Washington, Seattle, WA, USA, [2]Cooperative Institute for Research in Environmental Sciences, University of Colorado Boulder, Boulder, CO, USA, [3]Department of Geological Sciences, University of Colorado Boulder, Boulder, CO, USA

**Abstract** Strike-slip landscapes are often associated with a suite of characteristic geomorphic features that provide primary evidence for interpreting fault slip histories. Here we explore the role of shutter ridges, areas of relief advected laterally along faults, in generating two classic strike-slip processes: progressive lateral offset of channels and stream capture. Landscape models and comparative analysis of the Marlborough Fault System, NZ, show that the length of channel offsets observable in a landscape is primarily controlled by the length of shutter ridges. In our simple landscape model, this scale is controlled by the drainage spacing, and therefore by the geometry of the mountain range. In a more complex landscape, this scale may be controlled by lithologic or structural contrasts. We also find that shutter ridge relief inhibits stream capture, especially at slow fault slip rates relative to hillslope erosion rates. In this case, lateral drainage advection enables streams to "outrun" capture.

**Plain Language Summary** Many geoscientists look for horizontal stream deflection in a landscape in order to identify evidence of strike-slip faulting—a type of deformation that moves blocks of crust horizontally past one another. Based on results from this study, we suggest caution with this approach. Using a computer model of landscapes and comparison to the Marlborough Fault System of New Zealand, we determine that the "classic" signatures of strike-slip faulting, long stream channel offsets that flow parallel to the fault, and stream capture, which re-directs streams into neighboring channels, are controlled not by fault slip properties, such as slip rate or maturity, but by the presence and stature of shutter ridges (areas of high topography carried along the fault). In particular, we find that channel offset length is largely dictated by the length of the shutter ridge causing the obstruction. Stream capture rate is influenced by both length and height of shutter ridges, as well as fault slip rate and the rate at which the landscape is eroding. The bottom line from this study is that without topographic elements to impede the courses of streams, even a very long-lived and fast-slipping purely strike-slip fault may not develop and sustain long channel offsets.

## 1. Introduction and Background

Geomorphic features characteristic of strike-slip settings, such as linear, fault-parallel valleys, sag ponds, shutter ridges, elongated, offset, and warped stream channels, and laterally offset glacial moraines and river terraces, have long aided in the identification and study of strike-slip fault systems (e.g., Arrowsmith & Zielke, 2009; Jiang et al., 2017; Walker & Allen, 2012; Walker & Jackson, 2002; Wallace, 1949, 1968), including estimation of fault slip rates and off-fault deformation rates (Fu et al., 2005; Goren et al., 2015; Gray et al., 2017; Pucci et al., 2008; Replumaz et al., 2001; Sieh & Jahns, 1984). Despite this widely recognized suite of "classic" strike-slip landscape features, one key observable yet to be addressed carefully in the literature is that not all strike-slip faults, even the longest and fastest slipping among them, demonstrate consistently similar geomorphology. For example, Gaudemer et al. (1989) found that only 30% of channels crossing segments of the San Andreas Fault were offset in the "correct" direction, while Walker and Allen (2012) found a proportion of about 80% along the Kuh Banan Fault in Iran. Fu et al. (2005) observed that channel offset lengths across the Kunlun Fault in Tibet cluster around a few particular values. In order to successfully interpret landscapes for tectonic information, it is important to know what controls the topographic expression of a fault. Are tectonic variables such as slip rate, slip sense, and maturity most important? Or do characteristics of the surrounding landscape, such as topographic relief and relief structure, drainage density/spacing, slope angles, and bedrock erodibility dictate the near-fault landscape patterns?

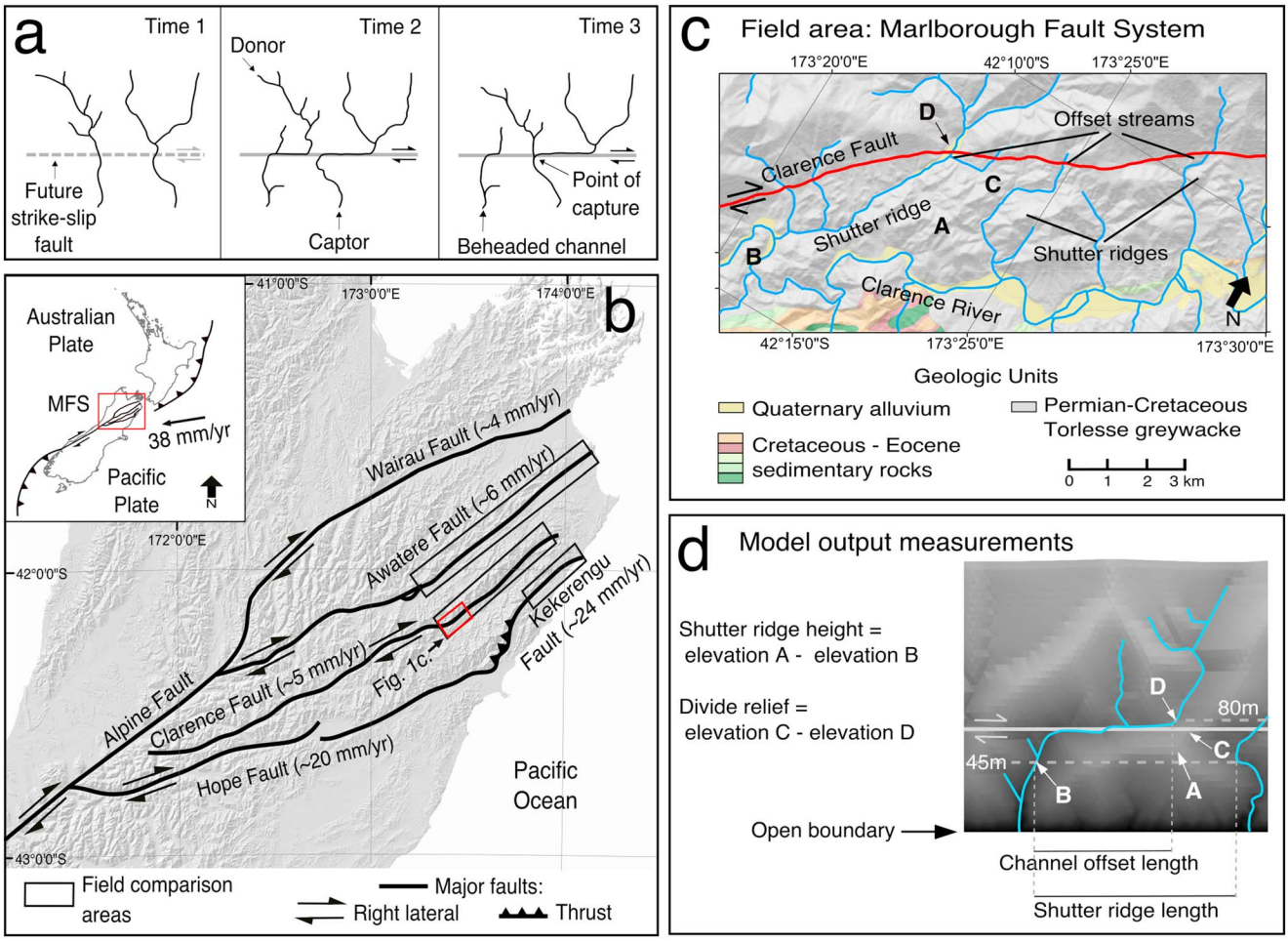


**Figure 1.** (a) The stream capture cycle. Time 1: Pre-strike-slip fault; streams flow straight across the future fault. Time 2: Right-lateral slip offsets streams and juxtaposes lower reaches of captor streams with upper reaches of eventual donors. Time 3: Stream capture. The cycle of offset and capture continues with fault activity. (b) Map of Marlborough Fault System (MFS), New Zealand. Inset map shows plate tectonic setting. Black boxes in main map show analyzed sections of strike-slip faults. Fault slip rates from Wairau (Zachariasen et al., 2006), Awatere (Little et al., 1998), Clarence (Knuepfer, 1992), Hope (Van Dissen & Yeats, 1991), and Kekerengu (Little et al., 2018). (c) Example of offset streams along the Clarence Fault. Geology simplified from Rattenbury et al. (2006). A, B, C, and D correspond to A, B, C, and D in panel d. (d) Model output measurements. Shutter ridge length: horizontal distance between adjacent streams at 45 m above the open boundary. Channel offset length: Horizontal distance between a stream's position at 80 m (4 m above the fault) and its position at 45 m. Shutter ridge height: Difference between the highest elevation on a shutter ridge, anywhere between the open boundary and 70 m from it, and elevation of the stream at 45 m. Divide relief: Elevation difference between the stream at its point of inflection, where it turns from flowing toward the fault to flowing parallel to the fault, and the point where the smallest amount of relief separates it from the captor stream.

Previous studies of streams that cross strike-slip faults demonstrate an ongoing cycle of fault-parallel channel lengthening by offset, followed by shortening of fault-parallel river segments by stream capture, as in Figure 1a (Duvall & Tucker, 2015; Gaudemer et al., 1989; Goren et al., 2014; Huang, 1993; Hubert-Ferrari et al., 2002; Ouchi, 2004, 2005; Replumaz et al., 2001; Wallace, 1968). These two processes have opposing effects on horizontal channel offset lengths—a measure of the "strength" of the landscape signature of strike-slip faulting—that can be observed at any snapshot in time. With each stream capture, apparent offset on a stream channel will be reduced or erased even as total offset on the fault continues to accumulate (Keller et al., 1982; Replumaz et al., 2001; Walker & Allen, 2012; Walker & Jackson, 2002; Wallace, 1968). Because geomorphology often provides the first line of evidence as to a fault's activity, slip rate, slip sense, or even existence, we must thoroughly understand the landscape characteristics that influence the expression of distinctive strike-slip features. At present, we lack studies that specifically address why classic strike-slip features, such as long stream offsets or occurrences of stream capture, exist in some places but not in others.

Here we examine modeled landscapes and the dextral Marlborough Fault System of New Zealand (Figure 1b) to study the effects of shutter ridges, and their specific dimensions, on the length of channel offsets and on the frequency of stream capture in mountainous terrain, and compare these effects at a variety of fault slip rates. We define shutter ridges as relief elements of any shape that are advected along one side of a strike-slip fault. Shutter ridges by definition block and divert channels (Wallace, 1968) and thus could prove critical elements in setting the landscape response to strike-slip faulting. When formed from advected interfluves, they reflect the local drainage spacing, which in turn is set by the geometry of the range (Hovius, 1996). Their length could also be set by more resistant lithologies or structural elements such as pressure ridges. We find that this length scale, in turn, sets the length scale of along-fault stream channel offsets, regardless of total fault offset. This close correspondence is imposed by a regular cycle of stream capture; however, the presence of high-relief shutter ridges or the lateral migration of hillslopes near the fault can reduce or eliminate the likelihood of stream capture.

## 2. Methods

### 2.1. Landscape Model Setup

We use the Channel-Hillslope Integrated Landscape Development (CHILD) model, a landscape evolution model that simulates the development of 3-D topography given tectonic, climatic, and material properties (Tucker, 2012; Tucker et al., 2001). In this configuration of the model, hillslope erosion is modeled by nonlinear hillslope diffusion, and fluvial incision rate is proportional to unit stream power (Roering et al., 1999; Whipple & Tucker, 1999).

Our model setup broadly follows the methods of Duvall and Tucker (2015; details in the supporting information). In order to create conditions that allow stream capture, as in Figure 1a, we modeled an uplifting, one-sided mountain ridge cut by a strike-slip fault. We ran 21 simulations, varying the relative rock uplift rate on the downhill side of the fault ("below") between 0.2 and 1 mm/year, and the lateral fault slip rate between 1 and 10 mm/year to test a range of shutter ridge morphologies and fault slip scenarios (Table S1). Relative rock uplift rate on the uphill side of the fault ("above") stayed fixed at 1 mm/year. We model a creeping fault, rather than one subject to earthquakes of a characteristic offset length and recurrence interval, in order to focus on the effects of long-term deformation and offset.

In our simple landscape model, shutter ridges originate naturally as interfluves advect horizontally along the fault. Varying the rock uplift rate on the downhill side of the fault creates shutter ridges with different amounts of relief. The length scale of shutter ridges is set by the drainage spacing of the landscape, which arises from the dimensions of the model domain, natural variability within the model, and the uplift rate below the fault.

We tracked three evenly spaced individual shutter ridges per model run over a time interval equivalent to 750 m of cumulative slip (75,000–750,000 years, depending on slip rate), recording the number of times that stream capture breached each ridge. Measurements were made after an initial 250 m of right-lateral slip in order to exclude transience from the initiation of strike-slip motion. We tracked shutter ridges rather than individual streams because shutter ridges maintained a consistent size and morphology throughout each model run. Upper watersheds of streams in some model runs changed in size and shape as models progressed. The total number of stream captures that breached a ridge was converted to stream captures per meter of lateral fault slip for comparison of stream capture frequency among faults with different slip rates.

To examine controls on offset channel length, we measured the along-fault length of the channel offset by the fault, shutter ridge height and length, and relief of the divide between adjacent streams (Figure 1d) for the three shutter ridges, and for five additional streams spaced at a regular along-strike interval, at the beginning of and halfway through the period of record. We focus on determining which size dimensions of shutter ridges (length, height, and interfluve divide relief) play the strongest role in determining channel offset length. Height and divide relief account for how great an obstacle a shutter ridge presents to stream capture. Measuring both metrics allows assessment of the relative importance of absolute shutter height versus relief across the drainage divide in the river capture process. Fault-parallel channel offset length was measured between the stream's position at consistent distances from the open boundary (Figure 1d) that were chosen because they captured the extent of fault-related offset for most streams, in order to apply a consistent

standard to all modeled streams. We made measurements at regular time steps, rather than immediately before capture events, in order to replicate the real-world experience of viewing a landscape at only one random point in time.

### 2.2. Field Comparison: The Marlborough Fault System, New Zealand

The model results were compared to analogous sites in the Marlborough Fault System (MFS). The MFS comprises four major right-lateral strike-slip faults, with various slip rates and ages, at the obliquely convergent boundary between the Australian and Pacific Plates on the South Island of New Zealand (Figure 1b; e.g., Wallace et al., 2007; Yeats & Berryman, 1987). The bedrock in the MFS is mostly sandstone and mudstone of the Permian-Cretaceous Torlesse Supergroup (Rattenbury et al., 2006), but other, more resistant units are found in some parts of the field area (see supporting information for more field site details).

We analyzed 77 tributaries flowing across the Awatere, Clarence, and Kekerengu Faults (Figures 1b and 1c). These faults bound the southeast flanks of mountain ranges of significant relief, making them near-ideal sites to compare to our model experiments. Shutter ridges of different sizes formed from advected interfluves, like those in our model, exist throughout the MFS. Some shutter ridges form in less erodible lithologies and appear much longer than the surrounding drainage spacing (e.g., Figure S1). Evidence also exists in the field area for previous stream captures, mostly in the form of beheaded channels, though we cannot comprehensively quantify stream captures through time as we do with the numerical model. We measure channel offset lengths throughout the field area using DigitalGlobe satellite imagery viewed through Google Earth, a 15-m DEM (NZDEM SoS v1.0), and where available, 0.5-m LiDAR, to document channel offset length, shutter ridge length, shutter ridge height, and relief of divides between adjacent streams (Columbus et al., 2011; NSF OpenTopography Facility, 2016; University of Otago-National School of Surveying, 2011). Channel offsets in our field area are more variable in shape than those in our model. Many channels are offset diagonally, like those measured by Huang (1993) on the Yishi Fault, rather than exactly along the fault trace. We determine offset length by projecting the inflection point of the channel on each side of the offset to the fault, and measuring the along-fault distance between these points. While some authors (Fu et al., 2005; Huang, 1993) project the course of the stream on either side back to the fault, then measure the fault-parallel distance between these points, irregularity in the courses of MFS streams would cause such projections to introduce additional uncertainty.

### 2.3. Statistical Regressions

We performed simple and multiple linear regressions to assess which variables best predict channel offset length in the model and field data, and stream capture frequency in the model data. To calculate the contribution of each predictor variable to total model fit and assess statistical significance, we used the Relative Importance package in the R programming language for statistical computing (version 3.3.3) (Grömping, 2006; R Core Team, 2017). Specifically, we used the LMG method, which averages over all possible orderings of the predictor variables to assign relative importance (Lindeman et al., 1980). Channel offset length and stream capture frequency were considered separately.

## 3. Results and Analysis

### 3.1. Model Results

In general, the models demonstrate the expected cycle of steady channel lengthening with lateral fault offset, punctuated by abrupt shortening caused by stream capture (Figure 1d and Movies S2 and S3). In some model experiments in which the lateral slip rate is slow relative to the erosive response of the landscape, we observe lateral ridge migration as described by Duvall and Tucker (2015; Movie S3). Duvall and Tucker (2015) observed that, when hillslope erosion is fast relative to lateral fault slip, ridges migrate, allowing shutter ridges to maintain connectivity with interfluves on the opposite side of the fault. This connectivity is briefly broken when stream capture breaches the divide between adjacent streams but reestablishes as fault motion continues, allowing ridges to realign across the fault. In extreme cases, streams may evade capture temporarily or indefinitely as interfluves migrate in advance of captor streams (Movies S4 and S5). When the lateral slip rate is fast relative to hillslope erosion, topography on either side of the fault is relatively stable, and shutter ridges do not stay connected to topography across the fault (Movie S2).

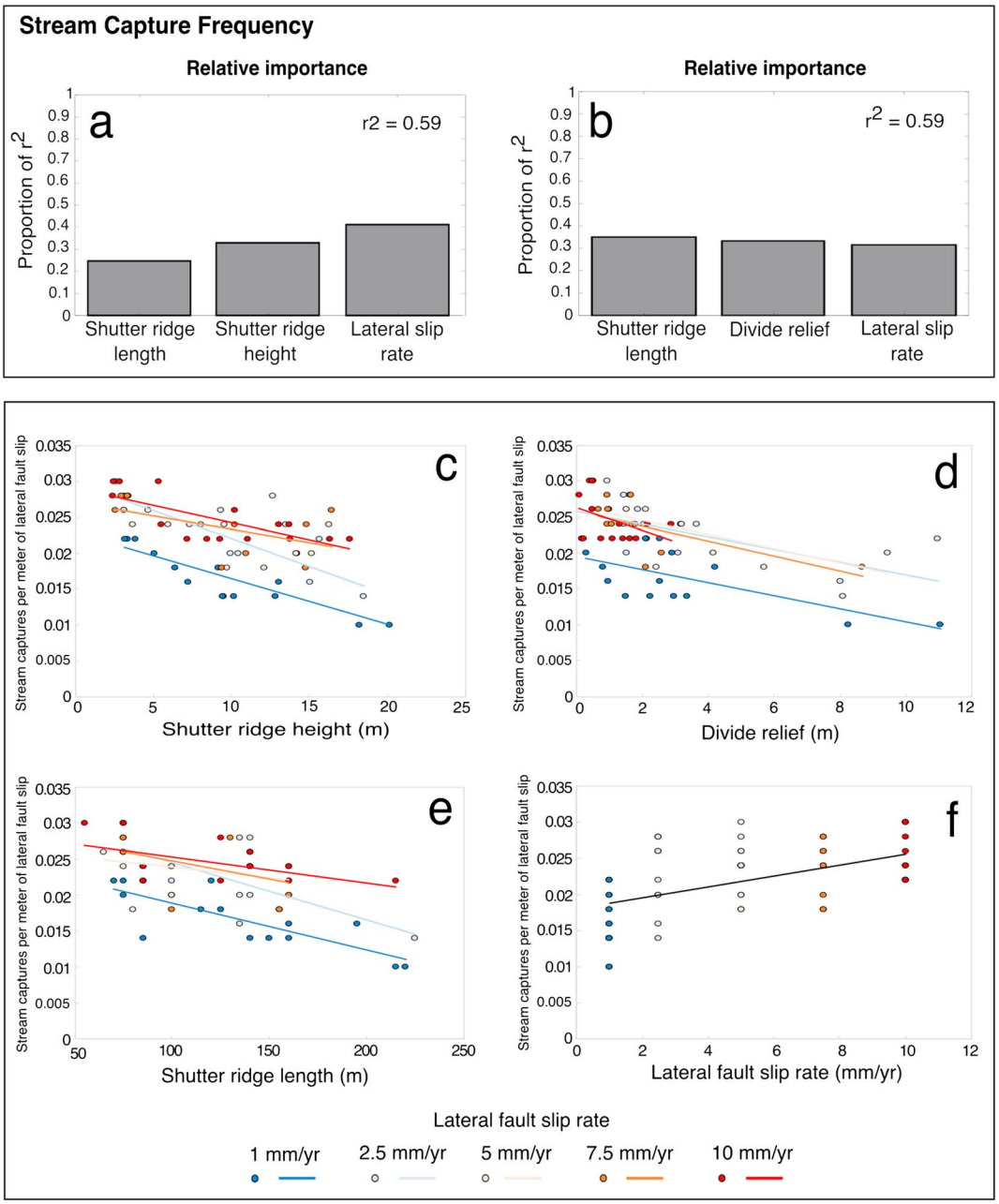


**Figure 2.** Model (left column) and field (right column) results for channel offset length. (a, b) Multiple linear regression models predicting channel offset length. Adjusted $r^2$ values shown for each regression. (c) Plot and simple linear correlations of channel offset length and shutter ridge length. The $r^2$ for trend lines are in Tables S3 and S5. Uncertainty on field measurements made from the NZDEM is approximately 15 m, and in those measurements made from the LiDAR, about 0.5 m, based on the resolution of the data. Additional, unquantified uncertainty likely arises from human measurement errors.

### 3.1.1. Channel Offset Length

Statistical regressions demonstrate the influence of shutter ridge length on channel offset length. Multiple linear regression models show that shutter ridge length dominates as the most important predictor of channel offset length, accounting for 70–90% of the model fit (adjusted $r^2$ = 0.70–0.80; $r^2$ throughout this paper refers to adjusted $r^2$; Figures 2a and 2b and Table S2). Simple linear regressions support this result, showing a strong correlation between the two lengths (Figure 2c and Table S3). Two measures of shutter ridge stature —height and divide relief—have a smaller and less robust correlation with channel offset length (Figures 2a,

2b, and Figure S2 and Table S3). Divide relief is a significant predictor of channel offset length and accounts for 8% of the model fit, whereas shutter ridge height is not a significant predictor. Shutter ridge height does account for 27% of the fit of the statistical model in which it was included (Figure 2a), but this correlation likely reflects a correlation between shutter ridge length and height, rather than an independent influence on channel offset length by shutter ridge height. Removing shutter ridge height from the regression does not substantially change the fit ($r^2$ = 0.66). Lateral fault slip rate is not a significant predictor of channel offset length, accounting for 1% or less of the fit in multiple regression models (Figures 2a and 2b and Table S2) and showing no meaningful correlation in simple regression plots (Figure S2 and Table S3).

#### 3.1.2. Stream Capture Rate

Statistical regressions demonstrate that shutter ridge dimensions and fault slip rate factor into the stream capture process. Multiple linear regression models show that all of the predictor variables play a roughly equal role in determining the rate of stream capture (Figures 3a and 3b and Table S2). Both multiple linear regression models fit the data fairly well, explaining about 60% of the variance ($r^2$ = 0.59). In these models, all variables were significant predictors of stream capture rate, and each accounted for 25–41% of the model fit. These results are supported by simple linear regression plots. Shutter ridge length and both measures of shutter ridge stature negatively correlate with stream capture frequency, with longer or taller ridges leading to less frequent stream captures (Figures 3c–3f and Table S3). Lateral fault slip rate has a modest positive correlation with stream capture rate, which is driven by the low stream capture rates in the slowest-slip models (Figure 3f).

### 3.2. Field Results

#### 3.2.1. Channel Offset Length

Multiple linear regression models of the MFS field data are consistent with model results: shutter ridge length is by far the most important predictor of channel offset length, contributing 72–90% of the model fit. The only other significant predictor in these models is divide relief, which contributes only 3% of the fit in the linear model that includes it as a predictor variable (Figures 2a and 2b and Table S4). Simple linear regressions of the MFS data show a positive correlation between channel offset length and shutter ridge length, shutter ridge height, and divide relief, with the strongest correlation being with shutter ridge length (Figures 2c and S3 and Table S5). The large Clarence River appears as an outlier in these results. With an offset of nearly 20 km, it likely records the entire offset of the Kekerengu Fault, thought to initiate only ~1 Ma (Wallace et al., 2007).

## 4. Discussion and Conclusions

Our work demonstrates the fundamental role that the presence (or absence) of shutter ridges plays in strike-slip fault landscapes. We found that the length of shutter ridges sets the scale of horizontally offset channels observed in a landscape, regardless of cumulative fault offset or fault slip rates (Figure 2). On the other hand, the topographic prominence of a shutter ridge, its lateral extent, and fault slip rate all impact rates of stream capture in a strike-slip landscape (Figure 3). These results confirm intuition that longer shutter ridges divert channels over greater distances and that taller/higher-relief shutter ridges act as greater barriers to stream capture. Less intuitively, shutter ridge length also affects the stream capture process because longer topographic obstacles juxtapose streams closely enough for capture less often.

Both shutter ridge height and divide relief reasonably predict stream capture occurrence, with a similar inverse linear relationship and moderate relative importance (Figures 3c and 3d). Shutter ridge height, which stays fairly consistent over time in our models, may serve as a better time-averaged representation of the height of obstruction. Divide relief changes over time as shutter ridges vary in degree of attachment to ridges above the fault, but likely serves as the best predictor of capture vulnerability at snapshots in time when adjacent streams have become closely juxtaposed. Stream capture acts to reduce the length of horizontally offset river channels, though temporarily. Therefore, the subtle correlations among shutter ridge height, divide relief, and channel offset length may be secondary effects of the stream capture process.

The models predict a weak positive relationship between fault slip rate and stream capture rate (Figure 3f). The models with conditions encouraging hillslope mobility—higher relative rock uplift and erosion rates, and smaller lateral slip rates (as expressed by advection-erosion number ($N_{ae}$) of Duvall & Tucker, 2015)—tend toward lower rates of stream capture. Streams in these cases can lose drainage area through

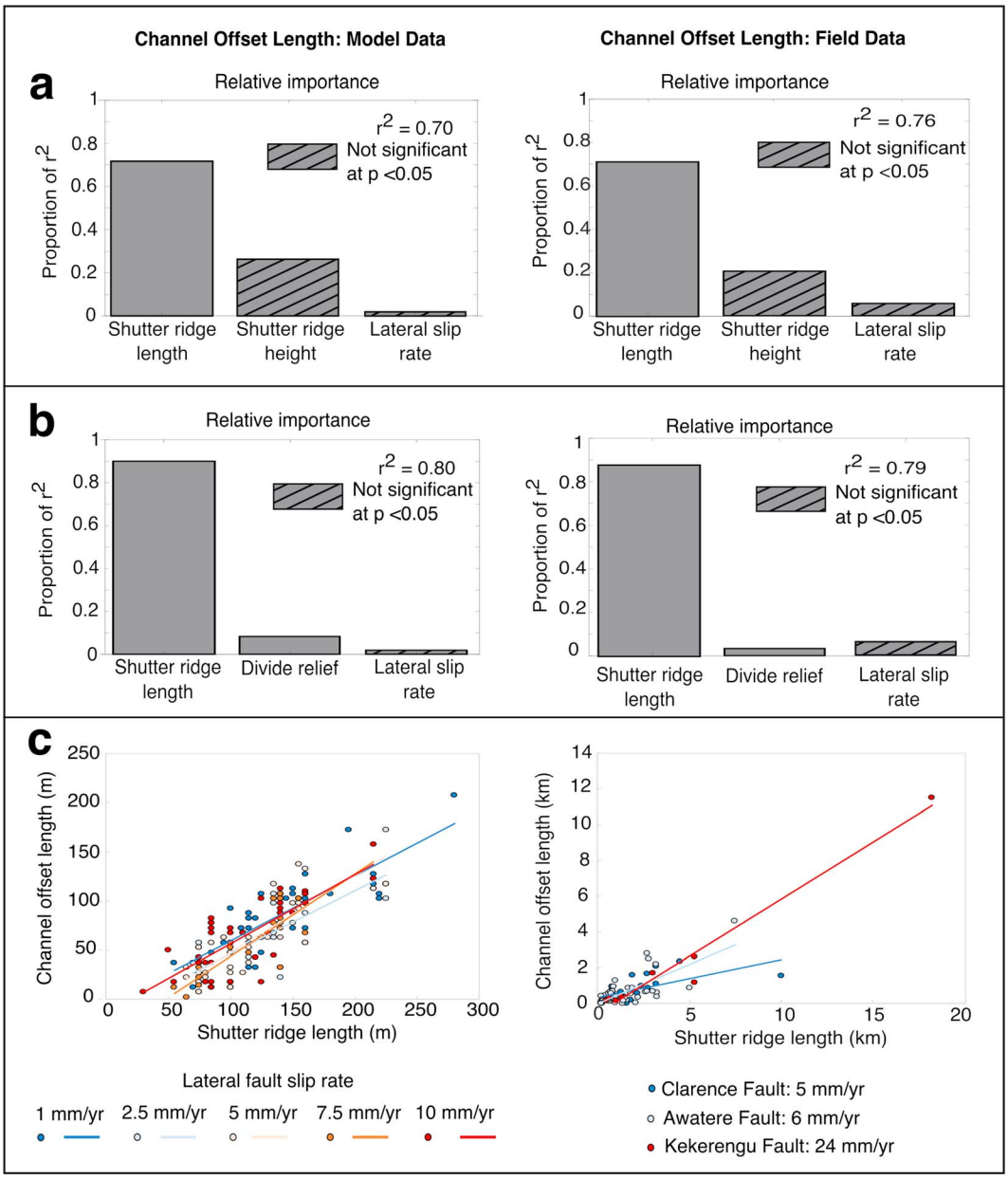


**Figure 3.** Model output results. (a, b) Multiple linear regression models predicting stream capture frequency. Adjusted $r^2$ values shown for each regression model. Plots and simple linear correlations of stream capture frequency and (c) shutter ridge height, (d) divide relief, (e) shutter ridge length, and (f) lateral slip rate. The $r^2$ for trend lines are in Table S3.

vigorous ridge migration rather than through stream capture, as entire watersheds translate laterally and "outrun" capture (Figure 4 and Movies S4 and S5). Thus, in certain circumstances, channel offsets shorter than the total fault offset can be maintained without stream capture.

Results from this study underscore the impact of the stream capture cycle, modulated by the presence and size of shutter ridges, in dictating whether strike-slip fault motion shows a clear geomorphic signature. In our simple landscape models, shutter ridges are advected interfluves with lengths set by drainage spacing, which in turn is set by the geometry of the mountain range (Hovius, 1996). As a result of the regular and effective process of stream capture in the models, as well as ridge migration in some cases, we also observe a close match between maximum magnitudes of channel offset length and shutter ridge length. As discussed above, shutter ridge height somewhat reduces stream capture, but, in general, once a stream becomes offset far

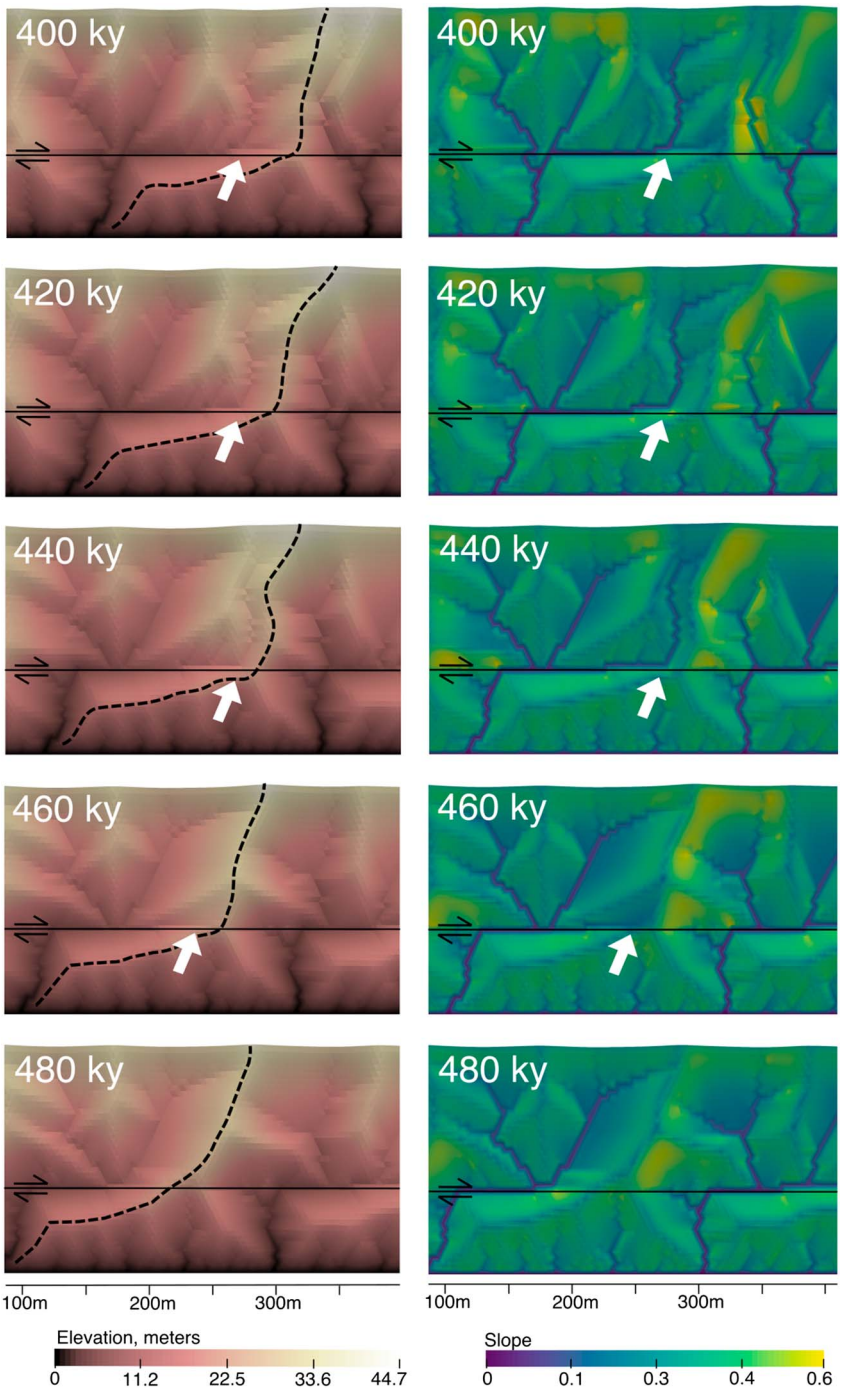


**Figure 4.** Channel-Hillslope Integrated Landscape Development (CHILD) model output showing a catchment "outrunning" capture through ridge migration. Dashed line shows drainage divide between left and right catchments. White arrows show tributary that is reduced in drainage area and ultimately defeated before it can be captured by the stream to the right.

enough to reach its neighbor, capture eventually occurs and prevents lengthening of the offset channel beyond the drainage spacing. We conclude that the surrounding landscape—the relief structure and drainage spacing that set up its shutter ridges—is primarily responsible for creating and maintaining the geomorphic signature of a strike-slip fault, whereas the fault properties are of lesser importance. In complex landscapes, erodibility contrasts or preexisting structural elements also create shutter ridges and set their length scales, and stream captures are not guaranteed even when two streams are juxtaposed in

close proximity. Questions surrounding how high and fast-moving advected topography must be relative to the efficiency of fluvial processes in order to become a true shutter ridge await future detailed studies.

Our work confirms that if fault-crossing rivers are positioned such that stream capture can occur, long channel offsets are better interpreted as transient features than as indicators of total fault offset (Walker & Allen, 2012). Evidence of a series of captures of a single stream, for example, a series of knickpoints (e.g., Prince et al., 2011; Yanites et al., 2013), could provide a longer record of slip on the fault than channel offset could. In cases of slow fault slip or highly erosive landscapes, hillslope migration could laterally advect entire streams without creating long offsets or easily allowing stream capture to occur, further dampening the landscape signature of the fault. In these cases, the profile relief ratio, suggested by Duvall and Tucker (2015) to assess ridge migration by determining the degree of ridge connectivity across the fault, may provide a good indicator of slip rate.

In all cases, a thorough understanding of the physical processes that control the occurrence of strike-slip features is essential to our predictive capability and our ability to read a particular landscape. Many geoscientists look for horizontal stream deflection as a litmus test for identifying the presence and sense of slip of a strike-slip fault. We suggest caution with this approach, as results from this study reveal the dependence of offset length on the preexisting scale of the landscape, and on the degree of hillslope mobility. Without topographic elements to impede the courses of streams, even a very long-lived and fast-slipping strike-slip fault may not develop and sustain long channel offsets.

**Acknowledgments**
We thank the National Science Foundation (EAR-1321859 and 1321735) and the University of Washington for support of this research. The CHILD model is distributed through the Community Surface Dynamics Modeling System (CSDMS) Model Repository, which is supported by NSF (EAR-1226297). Model input files are available in the supporting information. Feedback from Lindsay Schoenbohm and an anonymous reviewer improved this manuscript.

## References

Adams, C. J., Mortimer, N., Campbell, H. J., & Griffin, W. L. (2009). Age and isotopic characterisation of metasedimentary rocks from the Torlesse Supergroup and Waipapa Group in the central North Island, New Zealand. *New Zealand Journal of Geology and Geophysics*, *52*(2), 149–170. https://doi.org/10.1080/00288300909509883

Arrowsmith, J. R., & Zielke, O. (2009). Tectonic geomorphology of the San Andreas Fault zone from high resolution topography: An example from the Cholame segment. *Geomorphology*, *113*(1–2), 70–81. https://doi.org/10.1016/j.geomorph.2009.01.002

Baker, I. A., Gamble, J. A., & Graham, I. J. (1994). The age, geology, and geochemistry of the Tapuaenuku igneous complex, Marlborough, New Zealand. *New Zealand Journal of Geology and Geophysics*, *37*(3), 249–268. https://doi.org/10.1080/00288306.1994.9514620

Chappell, P. R. (2016). *The climate and weather of Marlborough*, *NIWA Science and Technology Series* (Vol. 69, 40 pp.). National Institute of Water and Atmospheric Research.

Columbus, J., Sirguey, P., & Tenzer, R. (2011). A free, fully assessed 15-m DEM for New Zealand. *Survey Quarterly*, *66*, 16–19.

Dolan, J. F. (2014). Data collection and processing report: LiDAR survey of five fault segments (Eastern Clarence, Western Clarence, Central Eastern Awatere, West Wairau and East Hope-Conway) of the Marlborough Fault System on the northwestern portion of New Zealand's South Island. National Center for Airborne Laser Mapping.

Duvall, A. R., & Tucker, G. E. (2015). Dynamic ridges and valleys in a strike-slip environment. *Journal of Geophysical Research: Earth Surface*, *120*, 2016–2026. https://doi.org/10.1002/2015JF003618

Fu, B., Awata, Y., Du, J., & He, W. (2005). Late Quaternary systematic stream offsets caused by repeated large seismic events along the Kunlun fault, northern Tibet. *Geomorphology*, *71*(3-4), 278–292. https://doi.org/10.1016/j.geomorph.2005.03.001

Gaudemer, Y., Tapponnier, P., & Turcotte, D. L. (1989). River offsets across active strike-slip faults. *Annales Tectonicoe*, *3*, 55–76.

Goren, L., Castelltort, S., & Klinger, Y. (2015). Modes and rates of horizontal deformation from rotated river basins: Application to the Dead Sea fault system in Lebanon. *Geology*, *43*(9), 843–846. https://doi.org/10.1130/G36841.1

Goren, L., Willett, S. D., Herman, F., & Braun, J. (2014). Coupled numerical–analytical approach to landscape evolution modeling. *Earth Surface Processes and Landforms*, *39*(4), 522–545. https://doi.org/10.1002/esp.3514

Gray, H. J., Shobe, C. M., Hobley, D. E., Tucker, G. E., Duvall, A. R., Harbert, S. A., & Owen, L. A. (2017). Off-fault deformation rate along the southern San Andreas Fault at Mecca Hills, southern California, inferred from landscape modeling of curved drainages. *Geology*, *46*(1), 59–62. https://doi.org/10.1130/G39820.1

Grömping, U. (2006). Relative importance for linear regression in R: The package relaimpo. *Journal of Statistical Software*, *17*(1), 1–27. https://doi.org/10.18637/jss.v017.i01

Hovius, N. (1996). Regular spacing of drainage outlets from linear mountain belts. *Basin Research*, *8*(1), 29–44. https://doi.org/10.1111/j.1365-2117.1996.tb00113.x

Huang, W. (1993). Morphologic patterns of stream channels on the active Yishi Fault, southern Shandong Province, Eastern China: Implications for repeated great earthquakes in the Holocene. *Tectonophysics*, *219*(4), 283–304. https://doi.org/10.1016/0040-1951(93)90179-N

Hubert-Ferrari, A., Armijo, R., King, G., Meyer, B., & Barka, A. (2002). Morphology, displacement, and slip rates along the North Anatolian Fault, Turkey. *Journal of Geophysical Research*, *107*(B10), 2235. https://doi.org/10.1029/2001JB000393

Jiang, W., Han, Z., Guo, P., Zhang, J., Jiao, Q., Kang, S., & Tian, Y. (2017). Slip rate and recurrence intervals of the east Lenglongling fault constrained by morphotectonics: Tectonic implications for the northeastern Tibetan Plateau. *Lithosphere*, *9*(3), 417–430. https://doi.org/10.1130/L597.1

Kamp, P. J., Vincent, K. A., & Tayler, M. J. (2015). Cenozoic sedimentary and volcanic rocks of New Zealand: A reference volume of lithology, age and paleoenvironments with maps (PMAPs) and database.

Keller, E. A., Bonkowski, M. S., Korsch, R. J., & Shlemon, R. J. (1982). Tectonic geomorphology of the San Andreas Fault zone in the southern Indio Hills, Coachella Valley, California. *Geological Society of America Bulletin*, *93*(1), 46–56. https://doi.org/10.1130/0016-7606(1982)93<46:TGOTSA>2.0.CO;2

Knuepfer, P. L. (1992). Temporal variations in latest Quaternary slip across the Australian-Pacific plate boundary, northeastern South Island, New Zealand. *Tectonics*, *11*(3), 449–464. https://doi.org/10.1029/91TC02890

Lindeman, R. H., Merenda, P. F., & Gold, R. Z. (1980). *Introduction to Bivariate and Multivariate Analysis*. Glenview, IL: Scott Foresman.
Little, T. A. (1995). Brittle deformation adjacent to the Awatere strike-slip fault in New Zealand: Faulting patterns, scaling relationships, and displacement partitioning. *Geological Society of America Bulletin*, *107*(11), 1255–1271. https://doi.org/10.1130/0016-7606(1995)107<1255:BDATTA>2.3.CO;2
Little, T. A., Grapes, R., & Berger, G. W. (1998). Late Quaternary strike slip on the eastern part of the Awatere fault, South Island, New Zealand. *Geological Society of America Bulletin*, *110*(2), 127–148. https://doi.org/10.1130/0016-7606(1998)110<0127:LQSSOT>2.3.CO;2
Little, T. A., Van Dissen, R., Kearse, J., Norton, K., Benson, A., & Wang, N. (2018). Kekerengu fault, New Zealand: Timing and size of Late Holocene surface ruptures. *Bulletin of the Seismological Society of America*, *108*(3B), 1556–1572. https://doi.org/10.1785/0120170152
Macara, G. R. (2016). *The climate and weather of Canterbury*, *NIWA Science and Technology Series* (2nd ed., Vol. 68, 44 pp.). Retrieved from https://www.niwa.co.nz/our-science/climate/publications/regional-climatologies/canterbury
NSF OpenTopography Facility (2016). Marlborough Fault System, South Island, New Zealand. https://doi.org/10.5069/g9g44n75
Ouchi, S. (2004). Flume experiments on the horizontal stream offset by strike-slip faults. *Earth Surface Processes and Landforms*, *29*(2), 161–173. https://doi.org/10.1002/esp.1017
Ouchi, S. (2005). Development of offset channels across the San Andreas Fault. *Geomorphology*, *29*(2), 161–173. https://doi.org/10.1002/esp.1017
Prince, P. S., Spotila, J. A., & Henika, W. S. (2011). Stream capture as driver of transient landscape evolution in a tectonically quiescent setting. *Geology*, *39*(9), 823–826. https://doi.org/10.1130/G32008.1
Pucci, S., De Martini, P. M., & Pantosti, D. (2008). Preliminary slip rate estimates for the Düzce segment of the North Anatolian Fault Zone from offset geomorphic markers. *Geomorphology*, *97*(3-4), 538–554. https://doi.org/10.1016/j.geomorph.2007.09.002
R Core Team (2017). *R: A language and environment for statistical computing*. Vienna, Austria: R Foundation for Statistical Computing. Retrieved from https://www.R-project.org/
Rattenbury, M. S., Townsend, D. B., & Johnston, M. R. (compilers) (2006). Geology of the Kaikoura area. (Sheet 70, scale 1:250,000, Geological Map 13.1). Lower Hutt, New Zealand: Institute of Geological and Nuclear Sciences GNS.
Replumaz, A., Lacassin, R., Tapponnier, P., & Leloup, P. H. (2001). Large river offsets and Plio-Quaternary dextral slip rate on the Red River fault (Yunnan, China). *Journal of Geophysical Research*, *106*(B1), 819–836. https://doi.org/10.1029/2000JB900135
Roering, J. J., Kirchner, J. W., & Dietrich, W. E. (1999). Evidence for nonlinear, diffusive sediment transport on hillslopes and implications for landscape morphology. *Water Resources Research*, *35*(3), 853–870. https://doi.org/10.1029/1998WR900090
Sieh, K. E., & Jahns, R. H. (1984). Holocene activity of the San Andreas Fault at Wallace Creek, California. *Geological Society of America Bulletin*, *95*(8), 883–896. https://doi.org/10.1130/0016-7606(1984)95<883:HAOTSA>2.0.CO;2
Tucker, G., Lancaster, S., Gasparini, N., & Bras, R. (2001). The channel-hillslope integrated landscape development model (CHILD). In *Landscape erosion and evolution modeling* (pp. 349–388). Boston, MA: Springer. https://doi.org/10.1007/978-1-4615-0575-4_12
Tucker, G. E. (2012). CHILD. Interdisciplinary Earth Data Alliance (IEDA). https://doi.org/10.1594/IEDA/100102
University of Otago-National School of Surveying (2011). NZ_SoS_DEM v1.0. University of Otago-National School of Surveying.
Van Dissen, R., & Yeats, R. S. (1991). Hope fault, Jordan thrust, and uplift of the seaward Kaikoura Range, New Zealand. *Geology*, *19*(4), 393–396. https://doi.org/10.1130/0091-7613(1991)019<0393:HFJTAU>2.3.CO;2
Walker, F., & Allen, M. B. (2012). Offset rivers, drainage spacing and the record of strike-slip faulting: The Kuh Banan Fault, Iran. *Tectonophysics*, *530-531*, 251–263. https://doi.org/10.1016/j.tecto.2012.01.001
Walker, R., & Jackson, J. (2002). Offset and evolution of the Gowk fault, SE Iran: A major intra-continental strike-slip system. *Journal of Structural Geology*, *24*(11), 1677–1698. https://doi.org/10.1016/S0191-8141(01)00170-5
Wallace, L. M., Beavan, J., McCaffrey, R., Berryman, K., & Denys, P. (2007). Balancing the plate motion budget in the South Island, New Zealand using GPS, geological and seismological data. *Geophysical Journal International*, *168*(1), 332–352. https://doi.org/10.1111/j.1365-246X.2006.03183.x
Wallace, R. E. (1949). Structure of a portion of the San Andreas rift in southern California. *Geological Society of America Bulletin*, *60*(4), 781–806. https://doi.org/10.1130/0016-7606(1949)60[781:SOAPOT]2.0.CO;2
Wallace, R. E. (1968). Notes on stream channels offset by the San Andreas Fault, southern Coast Ranges, California. In *Conference on geologic problems of the San Andreas Fault System*, *Geological Sciences* (Vol. 11, pp. 6–21). Stanford, CA: Stanford University Publications.
Wandres, A. M., & Bradshaw, J. D. (2005). New Zealand tectonostratigraphy and implications from conglomeratic rocks for the configuration of the SW Pacific margin of Gondwana. *Geological Society, London, Special Publications*, *246*(1), 179–216. https://doi.org/10.1144/GSL.SP.2005.246.01.06
Whipple, K. X., & Tucker, G. E. (1999). Dynamics of the stream-power river incision model: Implications for height limits of mountain ranges, landscape response timescales, and research needs. *Journal of Geophysical Research*, *104*(B8), 17,661–17,674. https://doi.org/10.1029/1999JB900120
Yanites, B. J., Ehlers, T. A., Becker, J. K., Schnellmann, M., & Heuberger, S. (2013). High magnitude and rapid incision from river capture: Rhine River, Switzerland. *Journal of Geophysical Research: Earth Surface*, *118*, 1060–1084. https://doi.org/10.1002/jgrf.20056
Yeats, R. S., & Berryman, K. R. (1987). South Island, New Zealand, and transverse ranges, California: A seismotectonic comparison. *Tectonics*, *6*(3), 363–376. https://doi.org/10.1029/TC006i003p00363
Zachariasen, J., Berryman, K., Langridge, R., Prentice, C., Rymer, M., Stirling, M., & Villamor, P. (2006). Timing of late Holocene surface rupture of the Wairau fault, Marlborough, New Zealand. *New Zealand Journal of Geology and Geophysics*, *49*(1), 159–174. https://doi.org/10.1080/00288306.2006.9515156
Zinke, R., Dolan, J. F., Van Dissen, R., Grenader, J. R., Rhodes, E. J., McGuire, C. P., Langridge, R. M., et al. (2015). Evolution and progressive geomorphic manifestation of surface faulting: A comparison of the Wairau and Awatere faults, South Island, New Zealand. *Geology*, *43*(11), 1019–1022. https://doi.org/10.1130/G37065.1